

Quantum chemical calculations of nuclear
spin-induced optical rotation in small organic
molecules

Eelis Kamula
Bachelor's thesis
Physics degree program
Faculty of science
University of Oulu
April 2021

Contents

1	Introduction	3
2	Theory	4
2.1	Quantum mechanics	4
2.1.1	Wave functions	5
2.2	Density functional theory	7
2.2.1	The variational principle	7
2.2.2	The Hohenberg-Kohn theorems	9
2.2.3	The Kohn-Sham method	11
2.2.4	Basis sets	12
2.2.5	Exchange-correlation functionals	13
2.3	Geometry optimization	14
2.4	Vibrational frequencies	14
2.5	Nuclear spin-induced optical rotation	14
2.5.1	Response functions	15
3	Quantum chemical calculations	16
3.1	Molecular structure preparation	17
3.2	Running the geometry optimization	17
3.3	Frequency calculation	19
3.4	Calculating nuclear spin-induced optical rotation	19
4	NSOR of model molecules	22
4.1	Objectives	22
4.2	Methods	22
4.3	Results	23
4.3.1	NSOR of ^{13}C	23
4.3.2	NSOR of ^1H	25
4.3.3	Comparison of ethanol and heptanol	26
4.4	Conclusions	27

1 Introduction

One of the best known methods to provide insight into the structure of materials is nuclear magnetic resonance spectroscopy, NMR spectroscopy for short [1]. Due to its versatility and non-invasivity NMR is one of the most popular methods out there. However, it is not the only method to examine materials because there are also many other spectroscopic methods such as infrared spectroscopy, Raman spectroscopy and ultraviolet-visible spectroscopy. All these spectroscopies give different information of the materials which is why it is meaningful having many kinds of them. There also exists a very specialized and new kind of method called nuclear magneto-optic spectroscopy, NMOS, and it has a lot of room for both theoretical and experimental development compared to other spectroscopic methods [2–6].

In NMR-spectroscopy, the magnetic moments of nuclei in a sample are oriented along the external magnetic field and they form a so-called bulk nuclear spin magnetization. To detect NMR signal, this magnetization vector needs to be flipped away from the direction of the main magnetic field. This can be done with a rotating magnetic field that is perpendicular to the direction of the external field. When rotating field is applied the magnetization vector starts precessing about it and it also precesses about the direction of the original external field. NMR signal is detected when the precession of the magnetization vector induces electric current to a coil [1]. In contrast to this, NMOS tries to examine how the magnetic moments in the sample change the polarization of light passing through the sample [2–6].

A few NMOS phenomena have been theoretically predicted [2–6] and one phenomenon has been experimentally detected. This detected phenomenon is called nuclear spin-induced optical rotation, NSOR [2]. Nuclear spin-induced optical rotation is an effect that occurs as a rotation of the plane of polarization of light as the light passes through a medium. This rotation occurs because light interacts with the magnetic moments in the sample. For NSOR it is important that the magnetic moments are oriented in a certain way with respect to the light beam since different orientations could lead to different NMOS effects [2–6].

NSOR can be mathematically expressed with a quadratic response function. In a general sense, response functions are used to describe change in expectation values of any observable or operator when external field is applied to the molecule. In optical spectroscopies this observable is dipole moment and the angle of the optical rotation can be expressed using a

quadratic response function which represents how the expectation value of the dipole of a molecule changes due to external fields. In the case of NSOR, these external fields are light and nuclear hyperfine interaction [7].

NSOR has been theoretically studied using quantum chemistry methods for a range of different molecules. These molecules include hydrocarbons, liquid and gaseous water, pyridine, pyrazine, xenon, nitromethane, urea, 11-*cis*-retinal protonated Schiff base, methyl alcohol, H₂ gas and graphene quantum dots [7–14]. Some general observations about the connection between molecular structure and corresponding NSOR response have been reported, such as existence of an optical chemical shift [7]. But despite being studied, the general rules between NSOR signal and molecular structure are not known and therefore the interpretation of experiments largely relies on theoretical calculations.

The goal of this thesis is to study the basic concepts of quantum chemistry, particularly Kohn-Sham density functional theory, and also to study how quantum chemical calculations and computation of nuclear spin-induced optical rotation can be done on a computer. Specifically, the calculations are done on small organic molecules.

2 Theory

2.1 Quantum mechanics

At the end of the 19th century, the main branches of physics seemed to give an explanation for all physical phenomena. The ability of the physical theories to interpret the experiments was such that many believed that all the fundamental laws of physics had been discovered and the task of physicists in the future would only be that of conducting more precise experiments. However, at the beginning of the 20th century certain experimental observations could not be explained with classical theories, some of the most famous being black body radiation and atomic spectra. It was these contradictions especially in atomic physics that forced physicists to develop new theories that were able to explain the experimental observations that disagreed with classical theories. In year 1900, Max Planck solved the black body radiation problem by suggesting that the energy of the radiation is not continuous but instead it consists of small units of energy called quanta. This led to the development of

completely new kind of physics called quantum mechanics. Quantum mechanical analysis becomes essential if the de Broglie wavelength of a system at hand is larger than or equal to the size of the system. The de Broglie wavelength is defined as $\lambda = h/p$ where h is the Planck constant and p is the momentum of the system. The de Broglie wavelength of everyday-sized objects is incredibly small and this is why the wave nature of everyday objects cannot be detected and classical mechanics describes these objects very accurately. But the de Broglie wavelength of atoms and molecules is about the same as their size, and quantum mechanics is needed to describe their behavior [15].

2.1.1 Wave functions

In classical mechanics a particle has well defined momentum and location in space. Together they completely and unambiguously determine the state of the particle. The time evolution of the state of the particle can be expressed using, for example, Hamilton's equations. If the location and momentum are known at some point in time, Hamilton's equations unambiguously determine the time evolution of the state of the particle and hence it is possible to predict what will happen to the particle in the future [15].

The transition from classical mechanics to quantum mechanics is as follows. Instead of using momentum or position in space we use a wave function $\Psi(\mathbf{r}, t)$ to describe the state of the particle. The time evolution of the state is not described by Hamilton's equations but, instead, by the Schrödinger equation

$$i\hbar \frac{\partial \Psi(\mathbf{r}, t)}{\partial t} = -\frac{\hbar^2}{2m} \nabla^2 \Psi(\mathbf{r}, t) + V \Psi(\mathbf{r}, t), \quad (2.1)$$

where ∇^2 is Laplacian and V is potential that the particle is subject to [15].

Classical mechanics explains things with complete precision but quantum mechanics is based on probabilities. Every particle is associated with a complex-valued wave function, $\Psi(\mathbf{r}, t)$, which represents all possible states of the particle. The product of the wave function and its complex conjugate, $\Psi(\mathbf{r}, t)\Psi^*(\mathbf{r}, t)$, represents a probability density for finding the particle from point \mathbf{r} at time t . Since wave functions are connected to probabilities, they have to be normalizable. All functions are not normalizable so only special kind of functions can be wave functions. These special kind of functions are called square-integrable functions

which means that the integral of the square of the absolute value of this kind of function over all space is finite. Together with inner product $\langle \cdot | \cdot \rangle$ the set of square-integrable functions form a so-called Hilbert space. Wave functions and, hence, all possible states of a particle are usually presented as quantum state vectors in Hilbert space

$$\Psi(\mathbf{r}, t) = \begin{bmatrix} r_1 \\ r_2 \\ \vdots \\ r_n \end{bmatrix} = |\Psi(t)\rangle \quad (2.2)$$

These vectors are called ket-vectors. Schrödinger equation takes the following form

$$\hat{H}|\Psi(t)\rangle = i\hbar \frac{\partial}{\partial t} |\Psi(t)\rangle, \quad (2.3)$$

where \hat{H} is Hamiltonian operator representing the total energy of the system. A wave function can be interpreted as a column vector or rather $n \times 1$ matrix and by taking a Hermitian transpose i. e. by taking a transpose and a complex conjugate of the vector $|\Psi(t)\rangle$, we get a so-called bra-vector

$$\Psi^\dagger(\mathbf{r}, t) = [r_1^* \quad r_2^* \quad \dots \quad r_n^*] = \langle \Psi(t) | \quad (2.4)$$

Often times in quantum mechanics we have to calculate expectation values of operators, for example the expectation value of the Hamiltonian of some system. Expectation value can be calculated by sandwiching the operator between bra- and ket-vectors

$$\langle \hat{H} \rangle = \langle \Psi(t) | \hat{H} | \Psi(t) \rangle = \int_{-\infty}^{\infty} \Psi^*(t) \hat{H} \Psi(t) d^3\mathbf{r} \quad (2.5)$$

It is important to understand that expectation value does not necessarily mean the most probable outcome of a measurement but instead it is understood as an average value of large number of measurements on identically prepared systems [15].

2.2 Density functional theory

All of the information in section 2.2 is from source [16].

Electrons carry elementary charge and they are constantly moving around nuclei in a molecule. Since they have electric charge, they are subject to Coulomb potential, interacting with each other and the nuclei. It should therefore be quite obvious that the electron system has a significant effect on molecular geometry. So, it is important to find out how the electron structure of the molecule affects the molecular geometry. One particularly good method for modeling the electron structure is density functional theory, DFT. It is a good method because it can give quite good results with relatively low computational costs.

Before going into details of DFT, it would be good to make clear the mathematical concept of a functional. Function is a mapping from one set to another that takes a single number as an argument and returns another number. Functional is similar, but instead of taking a single number as an argument it takes a function and returns a number. For example, if $f(x) = x^2$ and we choose $x = 2$, we get $f(2) = 2^2 = 4$. We can then define functional F that takes function $f(x)$ as an argument

$$F[f(x)] = \int_0^2 f^2(x) dx \quad (2.6)$$

Now, using the same function $f(x) = x^2$, we get

$$F[x^2] = \int_0^2 (x^2)^2 dx = \int_0^2 x^4 dx = \frac{32}{5} \quad (2.7)$$

2.2.1 The variational principle

All equations from now on are given in atomic units, where the charge of an electron e , its mass m_e , Dirac constant \hbar and the permittivity of the vacuum ε_0 multiplied by 4π , $4\pi\varepsilon_0$, have all been set to unity.

To be able to model the electronic structure of a molecule, we of course want to find a solution to the Schrödinger equation. The Hamiltonian for a molecule consisting of M

nuclei and N electrons can be written as

$$\hat{H} = -\frac{1}{2} \sum_{i=1}^N \nabla_i^2 - \frac{1}{2} \sum_{A=1}^M \frac{1}{M_A} \nabla_A^2 - \sum_{i=1}^N \sum_{A=1}^M \frac{Z_A}{r_{iA}} + \sum_{i=1}^N \sum_{j>i}^N \frac{1}{r_{ij}} + \sum_{A=1}^M \sum_{B>A}^M \frac{Z_A Z_B}{R_{AB}} \quad (2.8)$$

The indices A and B run over the M nuclei and i and j denote the N electrons. The first term describes the kinetic energy of the electrons and the second term the kinetic energy of nuclei. Here M_A denotes the mass of nucleus A . The third term is the attractive electrostatic interaction between the electrons and the nuclei, the fourth term is the repulsive potential due to electron-electron interaction and the last term is the repulsive potential due to nucleus-nucleus interaction. r_{pq} and R_{pq} are the distances between particles p and q . Since the electron is about 1836 times lighter than even the lightest of all nuclei, proton, the nuclei move way slower than the electrons. This means that we can approximate the nuclei to be fixed in space. This is called the Born-Oppenheimer approximation and the Hamiltonian (2.8) can be reduced to the so-called electronic Hamiltonian

$$\hat{H}_{elec} = -\frac{1}{2} \sum_{i=1}^N \nabla_i^2 - \sum_{i=1}^N \sum_{A=1}^M \frac{Z_A}{r_{iA}} + \sum_{i=1}^N \sum_{j>i}^N \frac{1}{r_{ij}} = \hat{T} + \hat{V}_{Ne} + \hat{V}_{ee} \quad (2.9)$$

Now the solution to Schrödinger equation is the electronic wave function Ψ_{elec} and electronic energy

$$\hat{H}_{elec} \Psi_{elec} = E_{elec} \Psi_{elec}. \quad (2.10)$$

No strategy to exactly solve this equation for molecular systems is known. Fortunately, there is a systematic way of approaching the ground-state wave function Ψ_0 , called the variational principle. The variational principle says that if we calculate the energy for any normalized wave function Ψ_{trial} , it will be an upper bound to the true ground-state energy, i. e.

$$\langle \Psi_{trial} | \hat{H} | \Psi_{trial} \rangle = E_{trial} \geq E_0 = \langle \Psi_0 | \hat{H} | \Psi_0 \rangle \quad (2.11)$$

This means that we can find the ground-state energy by minimizing the functional $E[\Psi]$. This can be done by searching through all continuous square-integrable N -electron wave

functions. Hence, E_0 can be expressed as

$$E_0 = \min\{E[\Psi]\} = \min\{\langle\Psi|\hat{H}|\Psi\rangle\} = \min\{\langle\Psi|\hat{T} + \hat{V}_{Ne} + \hat{V}_{ee}|\Psi\rangle\} \quad (2.12)$$

This kind of search through all possible wave functions is not possible in practice since there is a huge number of different wave functions. However, the wave functions can be divided into subsets and the best approximation to the exact wave function can be obtained from these subsets.

2.2.2 The Hohenberg-Kohn theorems

Since the way of exactly solving equation (2.10) remains unknown, we must find a new way of determining the energies of the electron system. Let us start by defining a new variable, the electron density $\rho(r)$, that determines the probability of finding any of the N electrons with an arbitrary spin from volume element dr_1 while the rest of the electrons have arbitrary spins and positions in the state Ψ

$$\rho(r) = N \int |\Psi(r_1, r_2, \dots, r_N)|^2 ds_1 dr_2 ds_2 \dots dr_N ds_N \quad (2.13)$$

Here, ds_i refer to spin coordinates. Now let's consider two different external potentials, V_{ext} and V'_{ext} , and assume that these potentials give rise to the same electron density $\rho(r)$. The Hamiltonians associated with these potentials are $\hat{H} = \hat{T} + \hat{V}_{ee} + \hat{V}_{ext}$ and $\hat{H}' = \hat{T} + \hat{V}_{ee} + \hat{V}'_{ext}$ and they are associated with ground-state wave functions Ψ and Ψ' and ground-state energies E_0 and E'_0 . If we use Ψ' as trial wave function for \hat{H} , by virtue of the variational principle we can write

$$\begin{aligned} E_0 &< \langle\Psi'|\hat{H}|\Psi'\rangle = \langle\Psi'|\hat{H}'|\Psi'\rangle + \langle\Psi'|\hat{H} - \hat{H}'|\Psi'\rangle \\ &= E'_0 + \langle\Psi'|\hat{T} + \hat{V}_{ee} + \hat{V}_{ext} - (\hat{T} + \hat{V}_{ee} + \hat{V}'_{ext})|\Psi'\rangle \\ &= E'_0 + \int \rho(r)(\hat{V}_{ext} - \hat{V}'_{ext}) dr \end{aligned} \quad (2.14)$$

Similarly, if the primed and the unprimed parts are interchanged, we get

$$E'_0 < E_0 - \int \rho(r)(\hat{V}_{ext} - \hat{V}'_{ext}) dr \quad (2.15)$$

Adding equations (2.14) and (2.15) together we get

$$E_0 + E'_0 < E'_0 + E_0 \implies 0 < 0 \quad (2.16)$$

Equation (2.16) is clearly a contradiction and hence, by *reductio ad absurdum*, we conclude that there cannot be two different external potentials that yield the same ground-state electron density. This means that the external potential is uniquely specified by the ground-state electron density and this is known as the first Hohenberg-Kohn theorem. The functional for the ground-state energy can be written as the sum of functionals of different components of the energy

$$\begin{aligned} E_0[\rho_0] &= E_{Ne}[\rho_0] + T[\rho_0] + E_{ee}[\rho_0] = \int \rho(r)V_{Ne} dr + T[\rho_0] + E_{ee}[\rho_0] \\ &= \int \rho(r)V_{Ne} dr + F_{HK}[\rho_0] \end{aligned} \quad (2.17)$$

Here $F_{HK}[\rho] = \langle \Psi | \hat{T} + \hat{V}_{ee} | \Psi \rangle$ is the Hohenberg-Kohn functional and it is same for all systems. The second Hohenberg-Kohn theorem says that $F_{HK}[\rho]$ gives the lowest energy of the system if and only if ρ is the true ground-state density ρ_0 . This can be proven using the variational principle. If $\tilde{\rho}$ is a trial electron density, $\tilde{\Psi}$ is the related wave function and $E_0 \leq E[\tilde{\rho}] = T[\tilde{\rho}] + E_{Ne}[\tilde{\rho}] + E_{ee}[\tilde{\rho}]$, we get

$$\langle \tilde{\Psi} | \hat{H} | \tilde{\Psi} \rangle = T[\tilde{\rho}] + V_{ee}[\tilde{\rho}] + \int \tilde{\rho} V_{ext} dr = E[\tilde{\rho}] \geq E_0[\rho_0] = \langle \Psi_0 | \hat{H} | \Psi_0 \rangle \quad (2.18)$$

This is the result we wanted because any trial electron density has to give an upper bound to the true ground-state energy. To summarize the Hohenberg-Kohn theorems

The ground-state energy from Schrödinger equation
is a unique functional of the electron density

The Hohenberg-Kohn theorems reduce even the biggest electronic-structure problems to

just three dimensions which is obviously a great thing when it comes to computational cost.

2.2.3 The Kohn-Sham method

The Hohenberg-Kohn theorems show that the electron density is an unambiguous quantity related to the ground-state of the system. However, the theorems provide no means whatsoever to finding the correct electron density. This is where the Kohn-Sham method comes into play. It provides a systematic way to find the correct density. Essentially the idea is to use a non-interacting reference system built from a set of one-electron orbitals and then the major part of the kinetic energy can be calculated to good accuracy and only a small part of the total energy has to be computed using an approximate functional. We start by defining a non-interacting system of N particles and we also define a local, effective potential $V_S(r)$ so that the electron density $\rho_S(r)$ obtained from the summation of the moduli of the squared spin orbitals exactly equals the ground-state density of the real system of interacting electrons

$$\rho_S(r) = \sum_i^N \sum_s |\phi_i(r, s)|^2 = \rho_0(r) \quad (2.19)$$

The spin orbitals ϕ_i are related to the probability of finding an electron with specific spin from a specific volume element. These spin orbitals are often referred to as the Kohn-Sham orbitals and they define the ground-state wave function of the non-interacting system. Equation (2.19) is the key part of the Kohn-Sham method because $V_S(r)$ has to be chosen so that the equation holds. The Kohn-Sham orbitals are determined by equations

$$\hat{f}^{KS} \phi_i = \varepsilon_i \phi_i \quad (2.20)$$

Operator \hat{f}^{KS} is called the one-electron Kohn-Sham operator and it is defined as

$$\hat{f}^{KS} = -\frac{1}{2} \nabla^2 + V_S(r) \quad (2.21)$$

It turns out that $V_S(r)$ has to be defined as

$$V_S(r) = \int \frac{\rho(r_2)}{r_{12}} dr_2 + V_{XC}(r_1) - \sum_A^M \frac{Z_A}{R_{1A}} \quad (2.22)$$

The first term is classical Coulomb potential and the last term is potential due to the nuclei. The second term is functional derivative of the so-called exchange-correlation energy $E_{XC}[\rho(r)]$ with respect to electron density

$$V_{XC} = \frac{\delta E_{XC}[\rho(r)]}{\delta \rho} \quad (2.23)$$

This exchange-correlation functional, or exchange-correlation potential, represents all unknown parts of the energy and it has to be approximated in practical quantum chemistry. When the potential $V_S(r)$ is calculated, it can be inserted to equation (2.21) and then the Kohn-Sham orbitals can be solved from equation (2.20). These orbitals are then inserted to equation (2.19) and we finally obtain the ground-state density and ground-state energy. The Kohn-Sham method is an iterative, self-consistent field procedure. This means that since the potential $V_S(r)$ already depends on density $\rho(r_2)$, the potential changes when the electron density is solved. This new density is then used in the next iteration and this continues until the input and output orbitals differ by less than a predetermined threshold. The Kohn-Sham orbitals can be solved using specific sets of functions called basis sets.

2.2.4 Basis sets

Solving the Kohn-Sham orbitals from equation (2.20) can be computationally really difficult so it is way more efficient to solve them approximately using a method called linear combination of atomic orbitals, LCAO. In LCAO method we have a set of predefined functions $\{\eta_\nu\}$ called basis functions. We can now express each Kohn-Sham orbital as a linear combination of these basis functions

$$\phi_i = \sum_{\nu=1}^L c_{\nu i} \eta_\nu \quad (2.24)$$

Here L is the number of basis functions in the basis set $\{\eta_\nu\}$. If we insert this into equation (2.20) and multiply from left with an arbitrary basis function η_μ and then integrate over all space we get

$$\sum_{\nu=1}^L c_{\nu i} \int \eta_\mu(r_1) \hat{f}^{KS}(r_1) \eta_\nu(r_1) dr_1 = \varepsilon_i \sum_{\nu=1}^L c_{\nu i} \int \eta_\mu(r_1) \eta_\nu(r_1) dr_1 \quad (2.25)$$

Here $i = 1, \dots, L$ so both integrals in these equations represent a matrix element of a specific $L \times L$ matrix. The integral on the left-hand side of the equation represents a matrix element of the Kohn-Sham matrix \mathbf{F}^{KS} and the integral on the right-hand side of the equation is a matrix element of overlap matrix \mathbf{S} . Coefficients $\{c_{\nu i}\}$ and orbital energies ε_i can also be represented with matrices \mathbf{C} and $\boldsymbol{\varepsilon}$ and so equation (2.25) can be written as a matrix equation

$$\mathbf{F}^{\text{KS}}\mathbf{C} = \mathbf{S}\mathbf{C}\boldsymbol{\varepsilon} \quad (2.26)$$

We see that with the LCAO method we have turned the difficult set of equations into a single matrix equation that can be rather easily solved with suitable computer programs. The bigger the basis set is, meaning the more basis functions there is, the better the approximations for Kohn-Sham orbitals are.

2.2.5 Exchange-correlation functionals

In equation (2.23) we encountered the exchange-correlation functional V_{XC} . Density functional theory is a general theory for calculating the electron density but it still needs this concrete functional to know how to treat the electron interactions - electron exchange and electron correlation. Electron correlation describes how the movement of one electron is influenced by all other electrons in the system. Electron exchange is purely quantum mechanical effect with no classical counterpart. If we have two identical fermions and we calculate the expectation value of the square of the distance between these fermions, we see that they are further away from each other than identical bosons. Since electrons are fermions, it seems like there is a repulsive force between these electrons. This quantum mechanical exchange effect arises from Pauli exclusion principle and the fermions' antisymmetric wave functions. The exchange-correlation functional tries to take these effects into account when we are calculating the ground-state energy [15]. There are many functionals of different types such as local density approximation (LDA), local spin-density approximation (LSDA), generalized gradient approximation (GGA), and there are also hybrid functionals where part of the exchange is calculated exactly using the Hartree-Fock method. One particularly well-performing functional is called B3LYP functional, which is a hybrid functional [16].

2.3 Geometry optimization

Before calculating molecular properties it is a common practice to optimize the molecular geometry. Geometry optimization is a procedure where wave functions and energy are computed for the initial guess of the geometry [17]. Then, the geometry is modified iteratively until an energy minimum is reached and intramolecular forces are below a defined threshold. The motivation behind geometry optimization is the physical significance of the optimized structure. Approximative quantum chemistry methods produce molecular geometries that are reasonably close to the geometries found in nature. The geometry can then be used for scientific research such as a starting point for theoretical studies of nuclear spin-induced optical rotation in small organic molecules.

2.4 Vibrational frequencies

Usually after molecular geometry is optimized using, for example, density functional theory, we want to see if the geometry minimum is actually reached. Sometimes quantum chemistry programs can optimize the geometry such that we reach, for example, a transition state, not the ground-state. The geometry minimum can be verified by calculating vibrational frequencies. Vibrational frequencies are essentially second derivatives of the total energy with respect to cartesian coordinates. Usually vibrational frequencies are given in wavenumbers and units are cm^{-1} . Sometimes after optimization some frequencies might be negative which means that some coordinate is at local maximum. When all frequencies are non-negative, the geometry minimum is reached [16].

2.5 Nuclear spin-induced optical rotation

Nuclear spin-induced optical rotation, NSOR for short, is a nuclear magneto-optic effect that occurs as a rotation of the plane of polarization of light when the light passes through a medium. Since change in polarization state of the light passing through a sample is induced by nuclear magnetic moments in the sample and interactions between the nuclei and the light are mediated by the electron cloud of the molecule [2], we can express many spectroscopic properties as perturbations in the electron system induced by external fields. This is also the case with nuclear spin-induced optical rotation. We can express NSOR in

terms of a quadratic response function, which introduces second-order correction to electric dipole of the molecule due to perturbation by light and nuclear hyperfine interaction of the molecule [12].

2.5.1 Response functions

The goal is to find out how the system at hand responds to light and hyperfine interaction perturbation. To do this we can utilize response functions. The goal of a response function is to find out how a system reacts to external fields and this is done by calculating time-dependent expectation value of an appropriate observable $\hat{\Omega}$ [18]

$$\begin{aligned}
\langle \Psi(t) | \hat{\Omega} | \Psi(t) \rangle &= \langle \Psi^{(0)} | \hat{\Omega} | \Psi^{(0)} \rangle \\
&+ \langle \Psi^{(1)} | \hat{\Omega} | \Psi^{(0)} \rangle + \langle \Psi^{(0)} | \hat{\Omega} | \Psi^{(1)} \rangle \\
&+ \langle \Psi^{(2)} | \hat{\Omega} | \Psi^{(0)} \rangle + \langle \Psi^{(1)} | \hat{\Omega} | \Psi^{(1)} \rangle + \langle \Psi^{(0)} | \hat{\Omega} | \Psi^{(2)} \rangle \\
&+ \dots
\end{aligned} \tag{2.27}$$

Here $|\Psi^{(n)}\rangle$ is nth order correction to the wavefunction. Equation (2.27) can also be written as

$$\begin{aligned}
\langle \Psi(t) | \hat{\Omega} | \Psi(t) \rangle &= \langle 0 | \hat{\Omega} | 0 \rangle \\
&+ \sum_{\omega_1} \langle \langle \hat{\Omega}; \hat{V}_\beta^{\omega_1} \rangle \rangle F_\beta^{\omega_1} e^{-i\omega_1 t} e^{\epsilon t} \\
&+ \frac{1}{2} \sum_{\omega_1 \omega_2} \langle \langle \hat{\Omega}; \hat{V}_\beta^{\omega_1}, \hat{V}_\gamma^{\omega_2} \rangle \rangle F_\beta^{\omega_1} F_\gamma^{\omega_2} e^{-i(\omega_1 + \omega_2)t} e^{\epsilon t} \\
&+ \dots
\end{aligned} \tag{2.28}$$

Here $\langle \langle \hat{\Omega}; \hat{V}_\beta^{\omega_1} \rangle \rangle$ is called linear response function and $\langle \langle \hat{\Omega}; \hat{V}_\beta^{\omega_1}, \hat{V}_\gamma^{\omega_2} \rangle \rangle$ is quadratic response function. \hat{V}^ω is a perturbation operator describing a small perturbation to the Hamiltonian of the system and it arises from interactions with electromagnetic fields. F^ω is the amplitude of an external field. Quantities ω_1 and ω_2 are angular frequencies of the external fields. Subscripts α , β and γ denote coordinate axes. Comparing equations (2.27) and (2.28) we can see that a first-order property of interest can be calculated as expectation value of the observable $\hat{\Omega}$ with respect to reference state $|0\rangle$. A second-order property is the

first-order correction to the expectation value of $\hat{\Omega}$ and it can be calculated from the first summation term in equation (2.28). A third-order property is the second-order correction to the expectation value of $\hat{\Omega}$ and it can be calculated from the second summation term in equation (2.28) [18].

Nuclear spin-induced optical rotation is a third-order property so it can be expressed using a quadratic response function with electric dipole and nuclear hyperfine interaction. Specifically, the angle of the optical rotation per unit length for plane-polarized light is [7]

$$\theta = -\frac{1}{12}\omega\mu_0c_0N_A I_K \varepsilon_{\alpha\beta\gamma} \Im \langle \langle \mu_\alpha; \mu_\beta, h_{K,\gamma}^{hf} \rangle \rangle_{\omega,0} \quad (2.29)$$

Here ω is the angular frequency of the incident light, μ_0 is permeability of vacuum, c_0 is speed of light in vacuum, N_A is the Avogadro constant, I_K is the spin of nucleus K and $\varepsilon_{\alpha\beta\gamma}$ is the Levi-Civita symbol. \Im indicates the imaginary part. The operators in the quadratic response function are the electric dipole $\hat{\boldsymbol{\mu}}$

$$\hat{\boldsymbol{\mu}} = -e \sum_i \mathbf{r}_i \quad (2.30)$$

and nuclear hyperfine interaction $\hat{\mathbf{h}}_K^{hf}$ which in non-relativistic theory corresponds to the paramagnetic spin-orbit operator $\hat{\mathbf{h}}_K^{PSO}$

$$\hat{\mathbf{h}}_K^{PSO} = \frac{e\hbar\mu_0}{4\pi m_e} \gamma_K \sum_i \frac{\mathbf{l}_{K,i}}{r_{K,i}^3} \quad (2.31)$$

Here e and m_e are the charge and mass of the electron, \hbar is Dirac constant, γ_K is gyromagnetic ratio of the nucleus K and $\mathbf{l}_{K,i}$ is the angular momentum of electron i in the vicinity of nucleus K [12].

3 Quantum chemical calculations

The theory presented in section 2 can be implemented on a computer using suitable computer programs such as Molden, Turbomole and DALTON. Molden is a pre- and post processing program for molecular and electronic structures and it can be used to build molecules [19]. Turbomole is a program for *ab initio* electronic structure calculations and it can be used

for many kinds of calculations for molecular systems. These include for example NMR shieldings, molecular dynamics, chemical reaction modeling, geometry optimization and also vibrational frequency calculations [20]. NSOR can be calculated for all nuclei in the molecule using DALTON which is a quantum chemistry program for calculating various molecular properties. DALTON is capable of standard tasks like geometry optimization and frequency calculations but it is also capable of calculating, for example, many types of molecular wave functions, potential energy surfaces, magnetic properties and polarizabilities [21].

3.1 Molecular structure preparation

Before performing quantum chemical calculations, the molecular structure has to be prepared and a convenient way to do this is to use a Z-matrix. A Z-matrix defines coordinates for all atoms in the molecule using the atoms' bond lengths, bond angles and dihedral angles which are often referred to as internal coordinates. Each line of a Z-matrix is constructed in the following manner [17]

Atom 1, Atom 2, Bond distance, Atom 3, Bond angle, Atom 4, Dihedral angle

However, on the first line there is only one atom since it is considered as a starting point and needs no coordinates. The position of the second atom can be described completely by a bond distance and the position of the third atom can be described by bond length and bond angle. All three coordinates are required to describe the fourth and subsequent atoms. A Z-matrix for methane would look like this

```
C
H 1 1.089000
H 1 1.089000 2 109.4710
H 1 1.089000 2 109.4710 3 120.0000
H 1 1.089000 2 109.4710 3 -120.0000
```

Bond distances are given in Ångströms which is a unit of length equal to 10^{-10} meters and angles are in degrees [17].

3.2 Running the geometry optimization

When a molecule is built using the Z-matrix editor, the molecular coordinates can be saved to a file as Cartesian coordinates. Turbomole uses its own kind of coordinate representation

so these Cartesian coordinates can be converted to coordinates in Turbomole format from Linux command line using Turbomole's command "x2t". Writing "x2t molecule.xyz > coord" Turbomole creates a file called coord that includes the coordinates in Turbomole format. The coordinates can then be used for preparing the input for geometry optimization. The input can be prepared using Turbomole's input generator called define [20].

There are four main menus in define module. The first main menu is the geometry main menu which allows one to build a molecule. We can give it commands "a coord" which adds atomic coordinates from file coord and "ired" which adds redundant internal coordinates. The second menu is the atomic attributes menu. There we can assign atomic basis set using command "b all def-TZVP". This means that we use def-TZVP basis set [22] for all nuclei in our molecule. Def-TZVP is a well-performing basis set and it stands for triple zeta valence with polarization functions. The third menu is the occupation numbers and start vectors menu. With command "eht" we can perform an extended Hückel calculation for the molecule. Extended Hückel calculation is a method that uses a linear combination of atomic orbitals method to calculate energies for molecular orbitals. The orbital energies from this calculation then provide occupation numbers and start vectors for our DFT calculations [20,23]. The last menu is the general methods menu. Here we can choose to use density functional theory for optimization calculations. Command "dft on" specifies that we want to use DFT and command "func b3-lyp" specifies that we want to use B3LYP exchange-correlation functional [24,25] for this calculation. The DFT calculations integrate the electron density on a numerical grid in space and coarseness of the grid affects the duration and precision of the calculation. We can specify the grid using command "grid m5" where m5 is the grid. This is a coarser grid but it is improved towards the end of the calculation [20]. The calculations can be significantly speeded up using a resolution of identity approximation. Resolution of identity is a way to approximate electron density by a linear combination of atom-centered auxiliary basis functions which have the same functional form as the usual basis functions used to describe molecular orbitals [26]. This makes the calculation much more efficient and it can be turned on with command "ri on". We can also write "dsp" which opens a submenu where we can turn on dispersion correction which takes into account long-range interactions between distant parts of the molecule [20,27]. After all the necessary information is selected and define session is ended, the program creates

files that contain all the information specified during the session and these files control the actions of other Turbomole programs. Now the geometry minimum can be calculated using command "jobex -ri" [20].

3.3 Frequency calculation

After optimization the geometry minimum can be verified with Turbomole program called aoforce. Aoforce is a module that calculates analytically harmonic vibrational frequencies for nuclei in the molecule. This calculation can be done with command "aoforce -ri". Aoforce program creates a file called vibspectrum which contains vibrational frequencies so when the calculation is finished the geometry minimum can be verified by checking that all the frequencies in that file are non-negative [28].

3.4 Calculating nuclear spin-induced optical rotation

After the geometry is optimized we can calculate NSOR for nuclei in the molecule. NSOR can be calculated in DALTON program. DALTON needs an input file from where the program executable reads the input containing methods, properties, parameters and everything else that has to be calculated. It also needs an input file for the molecule which contains information about the molecule. The desirable basis set is also specified in this file [21].

The input file for the molecule, from now on referred to as .mol-file, has a specific form. On the first line we write BASIS and on the second line we write the basis set we want to use. The third and the fourth line are comment lines but they can also be left blank. On the fifth line we can use keywords to write general instructions about the molecule. We have to specify how many different types of nuclei our molecule contains and this is indicated by the keyword Atomtypes. We can also specify number of symmetry generators and with keyword Integrals we can specify a threshold for which integrals smaller than this threshold will be considered to be zero. The rest of the .mol-file determines coordinates for nuclei in the molecule and also the proton number or charge of each nucleus is determined. So a .mol-file for a water molecule could look like this

BASIS

co2

```

Atomtypes=2  Generators=0  Integrals=1.00D-15 Angstrom
Charge=8.0  Atoms=1
O          0.0000000000    -0.2249058930    0.0000000000
Charge=1.0  Atoms=2
H          1.4523499293    0.8996235720    0.0000000000
H          -1.4523499293    0.8996235720    0.0000000000

```

Here we have used co2 basis set [29] which is a completeness-optimized set developed and tested for calculating NSOR [14].

The second input file, here referred to as .dal-file, contains the keywords telling the DALTON program that we want to calculate NSOR. All .dal-files start with `**DALTON` and the input is case sensitive so that only upper-case characters will be recognized. On the second line we can write `.RUN RESPONSE` to specify that we want to calculate a response property. Generally speaking, the input is divided into four modules called `**INTEGRALS`, `**WAVE FUNCTIONS`, `**PROPERTIES` and `**RESPONSE`. In `**INTEGRALS` module we write `.DIPLN` to calculate dipole length integrals

$$\langle \chi_\mu | \mathbf{r} | \chi_\nu \rangle \quad (3.1)$$

We also write `.PSO` to calculate paramagnetic spin-orbit integrals

$$- \left\langle \chi_\mu \left| \frac{\mathbf{l}_K}{r_K^3} \right| \chi_\nu \right\rangle \quad (3.2)$$

Here K is the nucleus of interest. Next we can write `.SELECT` to select for which atoms in the .mol-file the integrals are calculated. The line after `.SELECT` contains the number of atoms selected and the line after that contains the atoms themselves selected in numerical order from the .mol-file.

Next is the `**WAVE FUNCTIONS` part and here we can run density functional theory

calculation with keyword `.DFT` and on the next line we can describe which functional we want to use. In this part we can make a submodule called `*SCF INPUT` and here we can specify a convergence threshold for energy gradient in DFT calculation as `.THRESHOLD`. We can also change the number of iterations for direct inversion in the iterative subspace, DIIS, by writing `.MAX DIIS ITERATIONS`. Direct inversion in the iterative subspace is a method for accelerating and stabilizing the convergence of electronic structure calculations [30]. In the `**WAVE FUNCTIONS` part we can also make a submodule called `*ORBITAL INPUT` where we can define an initial set of molecular orbitals. Here we can use keyword `.5D7F9G` to indicate that we want to delete unwanted components in cartesian d, f and g orbitals.

NSOR is calculated in the `**RESPONSE` part so we don't need the `**PROPERTIES` part here. `**RESPONSE` is the part where we can calculate many different electronic molecular response properties based on various wave function methods as well as time dependent Kohn-Sham density functional theory. In submodule `*QUADRA` we can calculate third-order properties as quadratic response functions, for example the quadratic response function part in equation (2.29). With keywords `.APROP`, `.BPROP` and `.CPROP` we can specify operators A , B and C in response function which is of the following form

$$\langle\langle A; B, C \rangle\rangle_{\omega_b, \omega_c} \quad (3.3)$$

Here the appropriate operators A and B are dipole moment operators and we give the x , y and z directions of the operators as `XDIPLN`, `YDIPLN` and `ZDIPLN`. Operator C is the paramagnetic spin-orbit operator PSO. With keywords `.ASPIN`, `.BSPIN` and `.CSPIN` we can give information about spin for the quadratic response calculation. Finally, the frequencies ω_b and ω_c can be specified as `.BFREQ` and `.CFREQ`. From equation (2.29) we can see that ω_c is zero. The other frequency, ω_b , is set to correspond to 405 nanometer light which in Hartree units is 0.1125021037. The `.dal`-file ends with `**END OF DALTON INPUT`. The calculation itself can be started by submitting a batch job script to supercomputer.

4 NSOR of model molecules

4.1 Objectives

Still in its infancy, nuclear magneto-optic spectroscopy has a broad room for both theoretical and experimental development and in spite of multiple studies on the subject [7–14] the general connection between chemical moieties in molecules and the corresponding NMOS response has not been well established for any nuclear magneto-optic effect. For this reason the interpretation of NMOS experiments still largely relies on full rigorous quantum chemical calculations. Hence, the main objective here is to study the nuclear spin-induced optical rotation in small organic molecules and we are especially interested in the change in the NSOR response when a functional group is attached to a hydrocarbon.

4.2 Methods

Quantum chemical calculations were carried out for a set of small linear organic molecules. The molecules are heptane, heptanoic acid, heptan-1-imine, heptan-1-amine, heptanal and 1-heptanol. The heptane works as a reference molecule. NSOR was calculated for all nuclei and the values from heptane were subtracted from the corresponding values in other molecules. This way we can see how the functional group affects the NSOR.

The molecules were built in Molden and the geometries were then optimized in Turbomole using density functional theory, def-TZVP basis set [22] and B3LYP functional [24,25]. The geometry minimum was verified by calculating harmonic vibrational frequencies in Turbomole. The NSOR parameters were calculated in DALTON using the quadratic response function formalism, BHandHLYP density functional [31] and co2 basis set [14]. All calculations were done in vacuum.

The NSOR signals are labelled based on the distance from a heteroatom in functional group. This is calculated in carbon bonds, i.e. how many carbon bonds away from the heteroatom the nucleus of interest is. Carbon makes four bonds in total so different carbons might have different number of hydrogens attached to them. Therefore the shifts in NSOR values from hydrogens are averaged so that we take an average from the shifts in NSOR values of hydrogens attached to a specific nucleus so we get a single value for all ^1H nuclei.

4.3 Results

In figures 1 and 2 the x -axis shows the change in NSOR induced by different functional groups. Units are $\mu\text{rad}\cdot\text{dm}^3/\text{mol}/\text{cm}$. In the following I shorten this as μrad but all values are normalized to concentration and nuclear polarization. In the case of carbons the y -axis shows the distance from the heteroatom in the functional group. The distance is calculated as the number of carbon bonds. In the case of hydrogens the y -axis indicates the carbon where the hydrogens are attached to. Different molecules are distinguished by different colors and shapes.

4.3.1 NSOR of ^{13}C

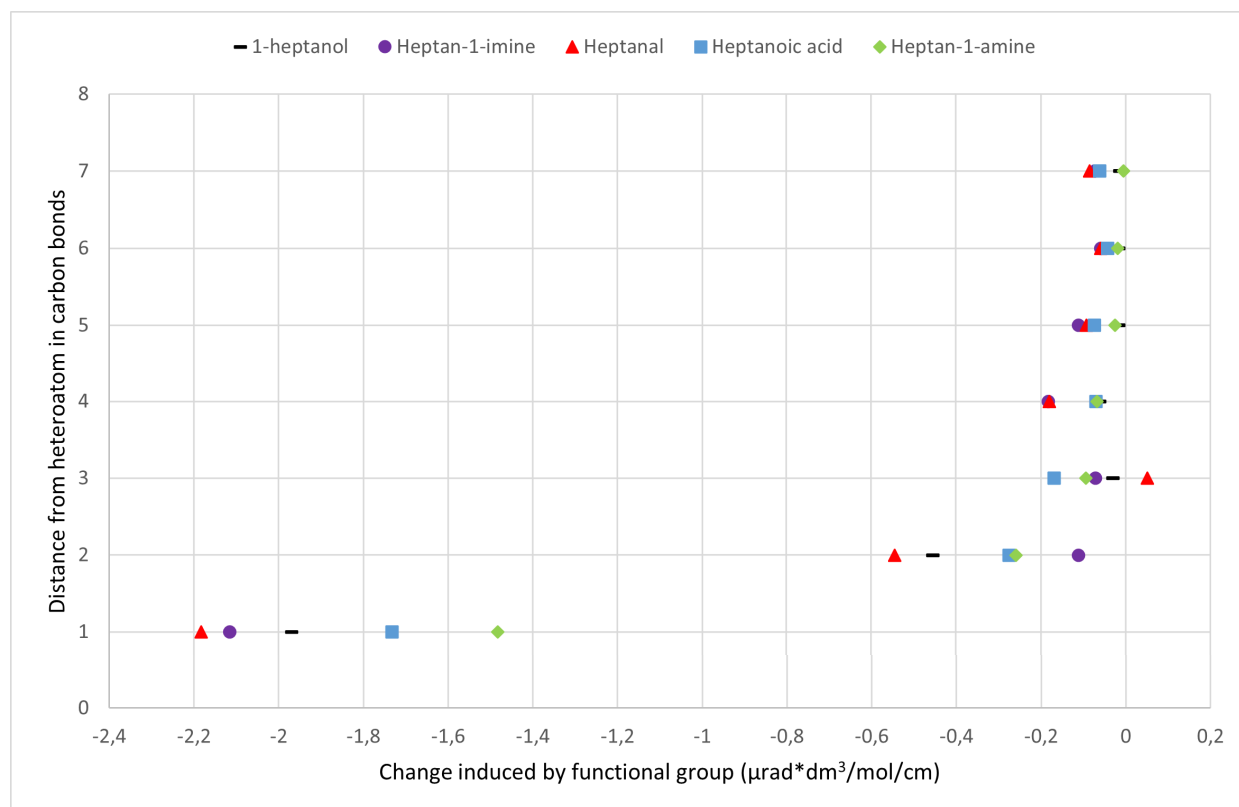


Figure 1: Change in ^{13}C NSOR induced by different functional groups. Black line is 1-heptanol, purple circle is heptan-1-imine, red triangle is heptanal, blue square is heptanoic acid and green diamond is heptan-1-amine. On the x -axis is the optical rotation and the y -axis shows the distance to the heteroatom.

In the case of carbon nuclei (Figure 1) the change in NSOR response right next to functional groups seems to be quite strong compared to the nuclei further away from the functional

groups. The values one carbon bond away from the heteroatom range from about $-1.5 \mu\text{rad}$ to about $-2.2 \mu\text{rad}$. Just one bond further the NSOR values are from about $-0.10 \mu\text{rad}$ to about $-0.55 \mu\text{rad}$ so the change is significantly smaller. There is still some variation three and four and even five bonds away but at distance of six bonds the change is already very small regardless of the functional group. Far away from the functional group the heptanoic acid, the imine and the heptanal induce somewhat equal change and also the heptanol and the amine induce somewhat equal change.

At almost all distances the aldehyde group seems to induce the strongest change in the NSOR. The alcohol group seems to induce one of the strongest changes but only up to the distance of two bonds. From three bonds on the change in NSOR of the alcohol group seems to remain almost constant but the aldehyde group has at least some variation at all distances. Comparing imine and amine, the imine group induces bigger change right next to the heteroatom but at distance of two bonds the value drops significantly. In the amine the change isn't so strong right next to the functional group. At distance of two bonds the NSOR response drops significantly, but not as much as in the imine. Three bonds and further than that the imine group still has some variance but the response of the amine group seems to remain closer to zero. The value of the heptanoic acid also drops significantly when moving from one bond to two bonds away, but it also has some variation at all distances.

Comparing oxygen groups and nitrogen groups, for example 1-heptanol and amine, the oxygen group induces stronger change at close distances. Further away from the functional group the changes even out and at four bonds and further than that it even seems like there is almost no difference at all between the heptanol and amine. This is also the case with heptanal and imine. The oxygen group induces a stronger change close to the functional group but further away the changes even out. The heptanoic acid contains oxygen and close to the functional group it induces a bigger change than the imine and the amine, except right next to the functional group it induces smaller change than the imine.

Close to the functional group there is some variation between different elements but further away they induce somewhat similar change. Four bonds away and further than that heptanol and amine have almost the same values and they have single bonds in functional groups. The same goes for functional groups with double bonds, heptanal, heptanoic acid and imine.

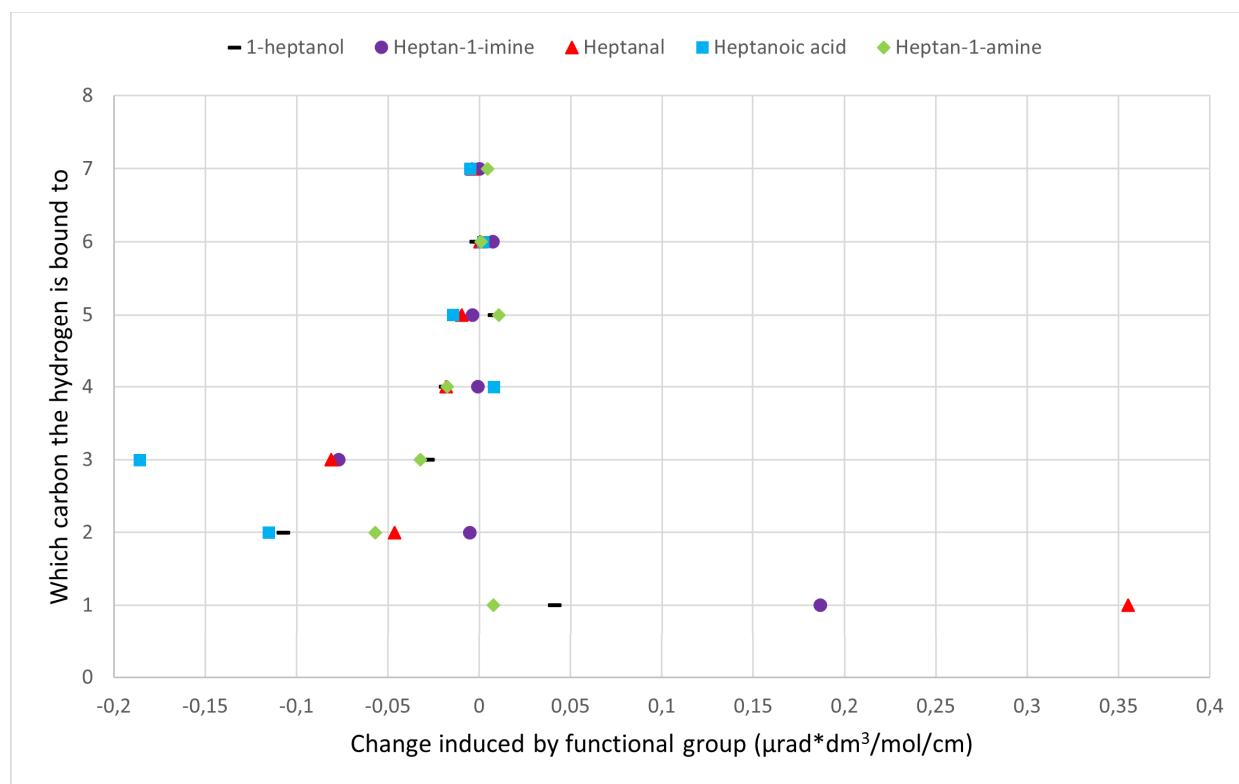
4.3.2 NSOR of ^1H 

Figure 2: Change in ^1H NSOR induced by different functional groups. Black line is 1-heptanol, purple circle is heptan-1-imine, red triangle is heptanal, blue square is heptanoic acid and green diamond is heptan-1-amine. On the x -axis is the optical rotation and the y -axis shows the distance to the heteroatom.

In the case of hydrogens (Figure 2) nuclei one to three carbon bonds away from the heteroatom have a large repertoire of NSOR values but at four bonds all values suddenly go to zero or almost zero. The amine group has the smallest variation and the heptanoic acid and the heptanal have the biggest variation close to the functional group. An interesting thing is that all shifts in the NSOR values next to the functional group are positive but at distance of two and three bonds the change in NSOR is negative for all nuclei. Overall the hydrogen values are smaller than the carbon values, ranging from $-0.19 \mu\text{rad}$ to about $0.36 \mu\text{rad}$.

The aldehyde induces much bigger change next to the heteroatom than the alcohol group. At distance of two bonds the aldehyde induces a smaller change but three bonds away it again induces bigger change. The same goes with the imine and the amine. The heptanoic acid induces the largest change at distance of two and three bonds. There is no hydrogen

one bond away for heptanoic acid because other nuclei already make four bonds with the carbon that is next to the heteroatom.

Comparing oxygen groups to nitrogen groups such as the heptanol to the amine, the oxygen group seems to induce bigger change in the vicinity of the functional group than the nitrogen group, but at large distances the changes even out. This is also the case with the heptanal and the imine. The heptanal induces bigger change close to the functional group but further away the changes even out again.

As in the case of carbons, also here different functional groups with single bond induce somewhat similar change especially at larger distances and so do different functional groups with double bonds. Closer to the functional group there is some variation between the NSOR values, but heptanol and amine have responses that are quite close to each other. Three bonds away and further than that the changes even out and the heptanol and the amine have almost the same NSOR response. This also goes with heptanal, heptanoic acid and imine. There is some variation but especially at larger distances these three have almost the same values. However, since there indeed is some variation in these changes in NSOR, it is not clear if this is a real trend or just a coincidence and further research is needed to get reliable information on the subject matter.

4.3.3 Comparison of ethanol and heptanol

Ikäläinen *et al.* studied NSOR in ethanol at the BHandHLYP/co-2 level of theory [7]. They used laser wavelength corresponding to about 0,093 Hartrees and I used wavelength corresponding to 0,113 Hartrees. Their wavelength is longer since smaller Hartree energy corresponds to longer wavelength. Here the changes in NSOR are not subtracted from the reference alkane but instead we use full NSOR values.

For oxygen they got a value of about $-23 \mu\text{rad}$ and I got about $-30 \mu\text{rad}$. For hydrogens bonded to oxygens the values are $0.10 \mu\text{rad}$ for ethanol and $0.14 \mu\text{rad}$ for heptanol. In methylene group the carbons have NSOR of $-1.30 \mu\text{rad}$ in ethanol and $-2.08 \mu\text{rad}$ in heptanol and the hydrogens have values $0.88 \mu\text{rad}$ in ethanol and $1.70 \mu\text{rad}$ in heptanol. Ethanol has a methyl group two bonds away from the oxygen but heptanol has methylene group because the carbon chain is much longer. However, it is interesting to compare these nuclei since they are at the same distance from the oxygen. The carbon in ethanol's methyl group has

NSOR of about $-0.46 \mu\text{rad}$ whereas carbon in heptanol's methylene group has NSOR value of $-2.40 \mu\text{rad}$. Hydrogens in these positions have values of $0.83 \mu\text{rad}$ in ethanol and $1.60 \mu\text{rad}$ in heptanol.

All NSOR responses in heptanol are larger than responses in ethanol. Oxygens have responses that are quite close to each other. An interesting thing is that in the case of carbons and hydrogens almost all values in heptanol are approximately two times larger than the values in ethanol. Exceptions are the carbon in ethanol's methyl group and the carbon in heptanol's methylene group. In ethanol this carbon is at the end of the chain and in heptanol the carbon is in the middle of the chain. This is probably one of the factors that explain the difference in NSOR responses. The other factor is that Ikäläinen *et al.* used different basis set which also has an effect on the response. For ethanol NSOR decreases at longer wavelengths which partly explains the ethanol's smaller NSOR values [7].

4.4 Conclusions

There are a few trends that show up with both carbons and hydrogens. The first trend is that nuclei close to the functional group have significantly bigger change in the NSOR value than nuclei further away from the functional group. The difference is most significant at one to three bonds away but it can still be seen at four and maybe even five bonds away from the functional group. Further than that all the differences in NSOR are quite close to zero. The second trend is that functional groups with double bonds induce bigger change than functional groups with single bonds. For example, heptanal induces bigger changes than 1-heptanol and imine induces bigger change than amine. Double bonds also create more variation in NSOR than single bonds. The main difference between carbons and hydrogens is that the change in NSOR is much stronger in carbons. The biggest change for carbons is almost $-2.18 \mu\text{rad}$. This is a significant change because it's about 20 times the value of the reference alkane which was $-0.11 \mu\text{rad}$. The biggest change for hydrogens is about $0.36 \mu\text{rad}$. This is about 20% increase to the response of the reference alkane which was $1.66 \mu\text{rad}$. The third trend is that oxygen has larger influence than nitrogen in the analogously bonded groups.

Given the fact that there is very limited set of data, the results can only be discussed

qualitatively and it is not possible to draw too many conclusions based on this study. However, it seems like nuclei in the vicinity of the functional groups are the most interesting ones and some functional groups might produce more interesting results than others. Especially functional groups including double bonds are interesting. It is clear that NSOR response is connected to chemical moieties in molecular structures and further research might reveal new information on the subject matter.

References

- [1] J. Keeler, “Understanding NMR spectroscopy (2004),” 2016.
- [2] I. Savukov, S. Lee, and M. Romalis, “Optical detection of liquid-state NMR,” *Nature*, vol. 442, no. 7106, pp. 1021–1024, 2006.
- [3] J. Vaara, A. Rizzo, J. Kauczor, P. Norman, and S. Coriani, “Nuclear spin circular dichroism,” *The Journal of Chemical Physics*, vol. 140, no. 13, p. 134103, 2014.
- [4] L.-j. Fu and J. Vaara, “Nuclear spin-induced Cotton-Mouton effect in molecules,” *The Journal of Chemical Physics*, vol. 138, no. 20, p. 204110, 2013.
- [5] L.-j. Fu and J. Vaara, “Nuclear spin-induced Cotton-Mouton effect in a strong external magnetic field,” *ChemPhysChem*, vol. 15, no. 11, pp. 2337–2350, 2014.
- [6] L.-j. Fu and J. Vaara, “Nuclear quadrupole moment-induced Cotton-Mouton effect in molecules,” *The Journal of Chemical Physics*, vol. 140, no. 2, p. 024103, 2014.
- [7] S. Ikäläinen, M. V. Romalis, P. Lantto, and J. Vaara, “Chemical distinction by nuclear spin optical rotation,” *Physical Review Letters*, vol. 105, no. 15, p. 153001, 2010.
- [8] P. Štěpánek, “Nuclear spin-induced optical rotation of functional groups in hydrocarbons,” *Physical Chemistry Chemical Physics*, vol. 22, no. 39, pp. 22 195–22 206, 2020.
- [9] J. Shi, S. Ikäläinen, J. Vaara, and M. V. Romalis, “Observation of optical chemical shift by precision nuclear spin optical rotation measurements and calculations,” *The Journal of Physical Chemistry Letters*, vol. 4, no. 3, pp. 437–441, 2013.
- [10] T. S. Pennanen, S. Ikäläinen, P. Lantto, and J. Vaara, “Nuclear spin optical rotation and Faraday effect in gaseous and liquid water,” *The Journal of Chemical Physics*, vol. 136, no. 18, p. 184502, 2012.
- [11] P. Štěpánek and A. M. Kantola, “Low-concentration measurements of nuclear spin-induced optical rotation using SABRE hyperpolarization,” *The Journal of Physical Chemistry Letters*, vol. 10, no. 18, pp. 5458–5462, 2019.

- [12] S. Ikäläinen, P. Lantto, and J. Vaara, “Fully relativistic calculations of Faraday and nuclear spin-induced optical rotation in xenon,” *Journal of Chemical Theory and Computation*, vol. 8, no. 1, pp. 91–98, 2012.
- [13] G. Yao, M. He, D. Chen, T. He, and F. Liu, “Analytical theory of the nuclear-spin-induced optical rotation in liquids,” *Chemical Physics*, vol. 387, no. 1-3, pp. 39–47, 2011.
- [14] J. Vähäkangas, P. Lantto, and J. Vaara, “Faraday rotation in graphene quantum dots: Interplay of size, perimeter type, and functionalization,” *The Journal of Physical Chemistry C*, vol. 118, no. 41, pp. 23 996–24 005, 2014.
- [15] J. Tuorila, “Quantum mechanics I,” 2017, University of Oulu, Lecture notes.
- [16] W. Koch and M. C. Holthausen, *A chemist’s guide to density functional theory*. John Wiley & Sons, 2015.
- [17] R. Withnall, B. Z. Chowdhry, S. Bell, and T. J. Dines, “Computational chemistry using modern electronic structure methods,” *Journal of Chemical Education*, vol. 84, no. 8, p. 1364, 2007.
- [18] P. Norman, K. Ruud, and T. Saue, *Principles and practices of molecular properties: Theory, modeling, and simulations*. Wiley Online Library, 2018.
- [19] G. Schaftenaar and J. H. Noordik, “Molden: a pre- and post-processing program for molecular and electronic structures,” *Journal of Computer-Aided Molecular Design*, vol. 14, no. 2, pp. 123–134, 2000.
- [20] “TURBOMOLE V7.5 2020, a development of University of Karlsruhe and Forschungszentrum Karlsruhe GmbH, 1989-2007, TURBOMOLE GmbH, since 2007; available from <https://www.turbomole.org>.”
- [21] K. Aidas, C. Angeli, K. L. Bak, V. Bakken, R. Bast, L. Boman, O. Christiansen, R. Cimiraglia, S. Coriani, P. Dahle, E. K. Dalskov, U. Ekström, T. Enevoldsen, J. J. Eriksen, P. Ettenhuber, B. Fernández, L. Ferrighi, H. Fliegl, L. Frediani,

- K. Hald, A. Halkier, C. Hättig, H. Heiberg, T. Helgaker, A. C. Hennum, H. Hettema, E. Hjertenæs, S. Høst, I.-M. Høyvik, M. F. Iozzi, B. Jansík, H. J. Aa. Jensen, D. Jonsson, P. Jørgensen, J. Kauczor, S. Kirpekar, T. Kjærgaard, W. Klopper, S. Knecht, R. Kobayashi, H. Koch, J. Kongsted, A. Krapp, K. Kristensen, A. Ligabue, O. B. Lutnæs, J. I. Melo, K. V. Mikkelsen, R. H. Myhre, C. Neiss, C. B. Nielsen, P. Norman, J. Olsen, J. M. H. Olsen, A. Osted, M. J. Packer, F. Pawłowski, T. B. Pedersen, P. F. Provasi, S. Reine, Z. Rinkevicius, T. A. Ruden, K. Ruud, V. V. Rybkin, P. Sałek, C. C. M. Samson, A. S. de Merás, T. Saue, S. P. A. Sauer, B. Schimmelpfennig, K. Sneskov, A. H. Steindal, K. O. Sylvester-Hvid, P. R. Taylor, A. M. Teale, E. I. Tellgren, D. P. Tew, A. J. Thorvaldsen, L. Thøgersen, O. Vahtras, M. A. Watson, D. J. D. Wilson, M. Ziolkowski, and H. Ågren, “The Dalton quantum chemistry program system,” *WIREs Comput. Mol. Sci.*, vol. 4, no. 3, pp. 269–284, 2014.
- [22] A. Schäfer, C. Huber, and R. Ahlrichs, “Fully optimized contracted gaussian basis sets of triple zeta valence quality for atoms Li to Kr,” *The Journal of Chemical Physics*, vol. 100, no. 8, pp. 5829–5835, 1994.
- [23] R. Hoffmann, “An extended Hückel theory. I. hydrocarbons,” *The Journal of Chemical Physics*, vol. 39, no. 6, pp. 1397–1412, 1963.
- [24] A. D. Becke, “Density-functional thermochemistry. III. The role of exact exchange,” *The Journal of Chemical Physics*, vol. 98, no. 7, pp. 5648–5652, 1993.
- [25] C. Lee, W. Yang, and R. G. Parr, “Development of the Colle-Salvetti correlation-energy formula into a functional of the electron density,” *Physical Review B*, vol. 37, no. 2, pp. 785–789, 1988.
- [26] R. Ahlrichs, “Efficient evaluation of three-center two-electron integrals over gaussian functions,” *Physical Chemistry Chemical Physics*, vol. 6, no. 22, pp. 5119–5121, 2004.
- [27] S. Grimme, “Semiempirical GGA-type density functional constructed with a long-range dispersion correction,” *Journal of Computational Chemistry*, vol. 27, no. 15, pp. 1787–1799, 2006.

-
- [28] P. Deglmann, K. May, F. Furche, and R. Ahlrichs, “Nuclear second analytical derivative calculations using auxiliary basis set expansions,” *Chemical Physics Letters*, vol. 384, no. 1-3, pp. 103–107, 2004.
- [29] P. Manninen and J. Vaara, “Systematic gaussian basis-set limit using completeness-optimized primitive sets. A case for magnetic properties,” *Journal of Computational Chemistry*, vol. 27, no. 4, pp. 434–445, 2006.
- [30] T. Rohwedder and R. Schneider, “An analysis for the DIIS acceleration method used in quantum chemistry calculations,” *Journal of Mathematical Chemistry*, vol. 49, no. 9, p. 1889, 2011.
- [31] A. D. Becke, “Density-functional exchange-energy approximation with correct asymptotic behavior,” *Physical Review A*, vol. 38, no. 6, p. 3098, 1988.